Influence of the Introduction of Short Alkyl Chains in Poly(2-(2-Thienyl)-1*H*-pyrrole) on Its Electrochromic Behavior

Cristina Pozo-Gonzalo,*,† Maitane Salsamendi,† José A. Pomposo,† Hans-Jurgen Grande,† Elena Yu. Schmidt,‡ Yu. Yu. Rusakov,‡ and Boris A. Trofimov‡

New Materials Department, CIDETEC—Centre for Electrochemical Technologies, Paseo Miramón 196, E-20009 Donostia-San Sebastián, Spain, and A. E. Favorsky Irkutsk Institute of Chemistry SB RAS, 1 Favorsky Str., 664033, Irkutsk, Russia

Received May 29, 2008; Revised Manuscript Received July 17, 2008

ABSTRACT: We report the significant effect of the introduction of short alkyl chains on the electrochromic behavior of poly(2-(2-thienyl)-1*H*-pyrrole), poly(**1**). Hence, poly(3-ethyl-2-(2-thienyl)-1*H*-pyrrole), poly(**2**), and poly(3-*n*-propyl-2-(2-thienyl)-1*H*-pyrrole), poly(**3**), presented multicolor electrochromism (both cathodic and anodic) exhibiting several colors: blue-grayish (+0.8 V), light blue (+0.2 V), light brown (0 V), brown (−0.1 V), dark orange (−0.2 V) and light orange (−0.8 V). Both poly(**2**) and poly(**3**) films showed a maximum optical contrast (ΔT_{max}) of ∼30% at a film thickness <100 nm. For both polymers, the optical responses for the oxidation and reduction process were in the range of a few seconds with a coloration efficiency during the bleaching process of 107−108 cm²/C. The new multichromic polymers were thermally stable up to 200 °C and showed reduced weight loss in the temperature range from 400 to 800 °C. The doping level for poly(**2**) and poly(**3**) was in the range of 26−31%. AFM images illustrated that poly(**2**) presented a much rougher surface than poly(**3**). The morphology corresponding to the oxidized state for both polymers was sharp, showing a significant smoothening of the surface upon reduction. Geometry optimizations and theoretical conformational analysis performed at the B3LYP/6-311G* level pointed to an increased population of *s-cis* conformers in **2** and **3** that presumably will be also retained in poly(**2**) and poly(**3**).

Introduction

Electrochromism is defined as the property inherent to some materials which can electrochemically switch between different colored states as a result of a redox reaction. Typical electrochromic behavior leads to switching between a transparent or bleach state and a colored state or between two different colored states.

Many different types of organic and inorganic materials such as inorganic metal oxides, mixed-valence metal complexes, organic small molecules and conducting polymers exhibit electrochromic behavior. Among the electrochromic materials, conducting polymers have received a great deal of attention due to outstanding electrochromic properties such as switching time, stability, coloration efficiency, or wide range of colors.

Of the conjugated electrochromic conducting polymers poly(3,4-ethylenedioxythiophene) (PEDOT)[1] and its derivatives are those that have been most extensively studied due to their suitability for various applications. These properties include high conductivity,[2] lower oxidation potentials compared to the neat polythiophene, and improved stability in its doped state. According to its electrochromic properties, PEDOT exhibits a transmissive oxidized state and a very absorptive neutral state which makes it suitable as an electroactive material in electrochromic devices.[3] Electrochromic materials present a broad range of applications such as electrochromic windows[4] and displays,[5] antiglare mirrors, eye-glasses or solar-attenuated windows.[6−10]

It is important to remark that although most electroactive polymers have the ability to exhibit two colors, only a few show multiple color states. Some strategies such as copolymerization and main-chain as well as pendant group structural modification have been followed in order to improve the electrochromic properties and achieve multichromic materials.[11]

For instance, electrochemical copolymerization of 2,2′-bis(3,4-ethylenedioxythiophene) (BiPEDOT) and 3,6-bis(2-(3,4-ethylenedioxy)thienyl-*N*-methylcarbazole (BEDOT-*N*MeCz) has been studied by Gaupp et al.[2] This research work revealed that by modification of the monomer ratios of BiPEDOT and BEDOT-*N*MeCz, during the electrochemical copolymerization, it is possible to obtain a broad color palette for a neutral polymer, but also for a given composition such materials showed electrochromic behavior (e.g., reddish-purple, blue and green). Similar studies have been performed by Varis et al.[11] by electrochemical copolymerization of 3,4-ethylenedioxythiophene (EDOT) and 1-(4-nitrophenyl)-2,5-di(2-thienyl)-1*H*-pyrrole (NTP) among others monomers.

Structural modification is also an interesting strategy in order to achieve materials with multichromic properties. For instance, in the literature there are several examples of polymers based on PEDOT derivatives like poly(bis-EDOT-pyridopyrazine)[12] which exhibits up to four different colors upon switching. Other examples, based on PEDOT derivatives, are poly[2,5-bis-(2,3-dihydrothieno[3,4-*b*][1,4]dioxin-5-yl)-pyridine], which presents a red neutral state, an oxidized blue-purple state, a reduced sky-blue state and a navy-blue protonated state, and poly[5,8-bis-(3-dihydrothieno[3,4-*b*][1,4]dioxin-5-yl)-2,3-diphenylpyrido[3,4-*b*]pyrazine], which exhibited several color changes upon doping: a neutral lime green, an oxidized light gray, a reduced burgundy red and a further reduced dark gray.[12] Argun et al.[13] have published an interesting review including different multicolored electrochromic copolymers based on PEDOT. Very recently, Kraft et al. have reported a new electrochromic polymer (*N*-ethyl substituted poly(3,4-ethylenedioxypyrrole)) which displays switching between green, violet and gray.[14]

Additionally, Song et al.[15] have reported an interesting strategy to achieve multicolor electrochromism from polypyrrole, by doping this conducting polymer with a molecular electrochromogen (2,2′-azinobis(3-ethylbenzothiazoline-6-sulfonate)).

* Corresponding author. E-mail: cpozo@cidetec.es.
† CIDETEC—Centre for Electrochemical Technologies.
‡ A. E. Favorsky Irkutsk Institute of Chemistry SB RAS.

10.1021/ma801190n CCC: $40.75
Published on Web 09/12/2008

Recently, we have reported dual orange-to-black electrochromic behavior in poly(2-(2-thienyl)-1*H*-pyrrole) electropolymerized from 2-(2-thienyl)-1*H*-pyrrole (**1**).[16] It should be noted that poly(2-(2-thienyl)-1*H*-pyrrole) was previously synthesized and characterized,[17−22] but attention was not paid to its electrochromic behavior. Such a property is useful for emerging flexible devices such as displays and variable optical attenuators.

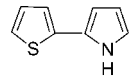

(1)

In this work we address the effect of the introduction of short alkyl chains in 2-(2-thienyl)-1*H*-pyrrole on the electrochromic behavior of the resulting polymers. It could be expected that electron-donating alkyl substituents in position 3 of the pyrrole ring will decrease the oxidative potential of the monomers, thus facilitating electropolymerization, and also they will distort the coplanarity of the monomers and hence of the resulting polymer chain. In other words, extra prerequisites for electrochromic behavior of the polymers existed in this case. Therefore, we have chosen ethyl and *n*-propyl substituents as those possessing moderate electronic and steric effect compared to bulkier and longer chain substituents.

As we will see in next sections, the resulting multichromic materials that show up to five different colors (dark orange, orange-yellowish, brown, blue and blue-grayish), are promising materials for organic electronic displays. Hence, an in-depth characterization of poly(3-ethyl-2-(2-thienyl)-1*H*-pyrrole), poly(**2**), and poly(3-*n*-propyl-2-(2-thienyl)-1*H*-pyrrole), poly(**3**), is performed including cyclic voltammetry, thermogravimetry, spectroelectrochemistry, colorimetry and atomic force microscopy measurements.

Scheme 1

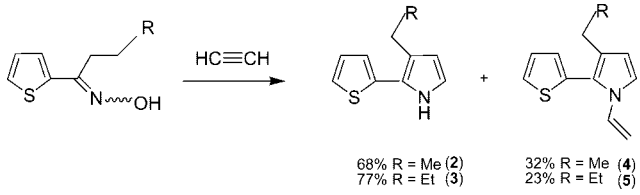

Results and Discussion

Synthesis of Monomers 2 and 3. The parent monomer, 2-(2-thienyl)-1*H*-pyrrole, **1**, was prepared and characterized as described in previous papers.[23,24] To the best of our knowledge, the work was the first where this monomer was synthesized and exhaustively described.[23] 3-Ethyl-2-(2-thienyl)-1*H*-pyrrole, **2**, and 3-*n*-propyl-2-(2-thienyl)-1*H*-pyrrole, **3**, were synthesized from 1-(2-thienyl)-1-butanone oxime and 1-(2-thienyl)-1-pentanone oxime and acetylene in the presence of the KOH/DMSO system using the modified Trofimov reaction (Scheme 1).[25−28] Details of the synthesis and monomer purification are reported in the Experimental Section.

Derivative **2** was previously prepared from 1-(2-thienyl)-1-butanone oxime and acetylene (atmospheric pressure, 100 °C, 7 h, 52% yield).[29,30] Later,[31] this monomer was also synthesized in the yield of 34% from 1-(2-thienyl)-1-butanone oxime and dichloroethane as synthetic equivalent of acetylene (NaOH, DMSO, 120 °C, atmospheric pressure, 7 h).

In this work, to optimize the reaction (to shorten reaction time and minimize KOH content) we have developed a pressure synthesis (acetylene under initial pressure 14 atm was used and the reaction was carried out in autoclave). Under pressure the solubility of acetylene in the reaction mixture and, hence, its concentration therein considerably increase, and therefore the reaction is progressively accelerated. As a result, the reaction time was 5−30 min instead of 7 h in the former work.

The milder temperature conditions and shorter reaction time as well as lower concentration of the strong base catalyst allow the monomer to be prepared in higher purity.

The mechanism of the pyrrole ring construction was proved[25] to involve the *O*-vinyl oxime prototropic isomerization to the vinyl ether of the hydroxyl amine derivative which further undergoes [3,3]-sigmatropic rearrangement to the imino aldehyde. The latter is ring-closed to the hydroxyl pyrroline, which further is dehydrated and aromatized to the pyrrole (Scheme 2).

Also the one-pot three-component version of this reaction (Scheme 3) starting directly from ketones, hydroxylamine and acetylene in the KOH/DMSO system elaborated recently has been significantly modified.[32,33]

Electrochemical Characterization of 2 and 3. The redox behavior of monomers **2** and **3** has been studied using cyclic voltammetry from a solution of 10^{-3} M substrate in dry acetonitrile and 0.1 M $LiClO_4$ as supporting electrolyte (vs Ag/AgCl). Under these conditions, both monomers gave two irreversible oxidation processes (Figure 1).

Both oxidation processes appear at similar values; for instance, the first oxidation process of **2** and **3** (E_{1ox} = +0.84 V and +0.80 V) presents a difference of ca. 40 mV, and the second oxidation process (E_{2ox} = +1.19 V and +1.18 V) occurs basically at the same value. These processes may be assigned to the oxidation of the pyrrole and thiophene rings, respectively. Electrochemical behavior of derivative **1** has been previously reported (E_{1ox} = +0.86 V and E_{2ox} = +1.30 V).[16] Derivatives **2** and **3** present a similar electrochemical behavior to **1**. Similar trends were found for short alkyl substituted 3,4-propylenedioxithiophene[34] and 3,4-ethylenedioxythiophene derivatives.[35]

Electropolymerization of 2 and 3 to Poly(2) and Poly(3). Both monomers **2** and **3** were electropolymerized, under the same conditions used for the cyclic voltammetry experiments, by repetitive potential scanning over the first oxidation process (from 0 to +1 V) at 50 mV/s leading to blue-grayish films on the working electrode.

Figure 2 displays the successful electropolymerization of **2** and **3** on a Pt working electrode where an increase in current is observed after successive scans. This effect is indicative of the deposition of an electroactive polymeric film on the electrode. Electrodeposition efficiency for poly(**2**) and poly(**3**) was studied by comparing the amount of electroactive polymer deposited with a set number of repeated scans.[36] The electrodeposition process of poly(**3**) occurs at a higher rate than poly(**2**) as it is observed for the anodic current response in Figure 2 leading to a more deep colored film.

In each case, prior to further characterization and to eliminate the possibility of charge trapping, the as-made polymers were completely dedoped in a 0.1 M $LiClO_4$ monomer-free acetonitrile solution. Cyclic voltammograms of films corresponding to the completely dedoped polymers were recorded in a monomer-free acetonitrile solution leading to a quasi-reversible oxidation process at +0.35 V for poly(**2**) and +0.32 V for poly(**3**) (Figure 3). The doping level determined as described by Arbizzani et al.[37] was found to be 31% for poly(**2**) and 26% for poly(**3**), which is common in conducting polymers.[38−41]

The redox processes of the polymers poly(**2**) and poly(**3**) appear at lower oxidation values than those corresponding to the monomer, as a consequence of the increase in conjugation along the polymeric chain.[42] Interestingly, dedoped poly(**1**) presents an oxidation process at +0.68 V (vs Ag/AgCl), which is higher than those for the polymers bearing ethyl and *n*-propyl side chains. For understanding of this behavior is important to evaluate both the electron donation and steric effect. In general,

Scheme 2

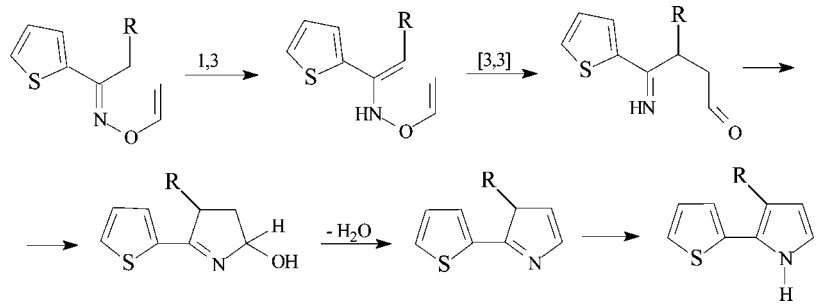

Scheme 3

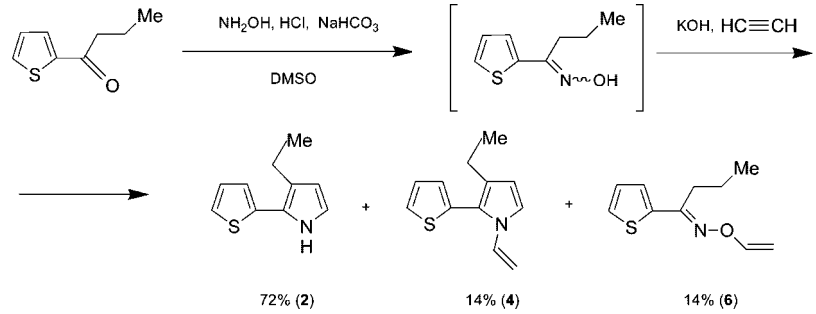

the electron donation of the side chain will reduce the oxidation potential (alkyl groups act as weak electron donors) but the steric effect will increase the oxidation potential. In our case, due to the length of the alkyl chain, the steric effect is not too notable and, therefore, the electron donation effect will be greater than the steric effect (the known linear correlations between the pKr value of substituted pyrroles with the inductive constant ε_I of the substituent in the pyrrole ring, including alkyls in position 3, supports this assumption),[43] leading to a reduction in oxidation potential.[44] A theoretical quantum chemical study is reported later supporting the experimental findings.

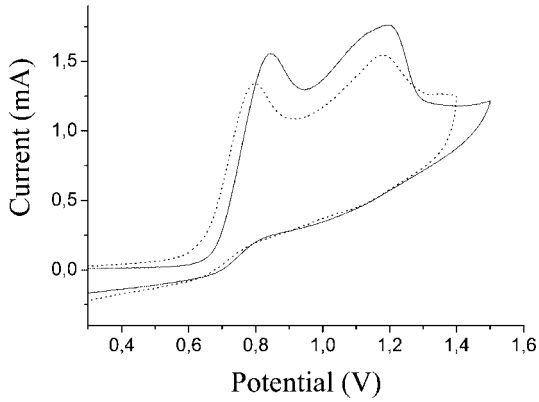

Figure 1. Cyclic voltammogram of monomer **2** (solid line) and **3** (dotted line) in acetonitrile; 10^{-3} M substrate, 0.1 M $LiClO_4$ using Pt sheet as working electrode and auxiliary electrode, and Ag/AgCl as reference electrode.

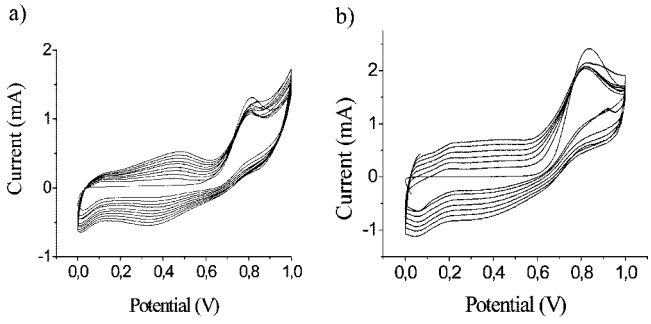

Figure 2. Electrodeposition of poly(**2**) (a) and poly(**3**) (b) on Pt sheet; Ag/AgCl as reference electrode and Pt sheet as counter electrode, 10^{-3} M acetonitrile solution of the substrate, 0.1 M $LiClO_4$ at a scan rate of 50 mV s^{-1}.

A linear relationship between the maximum peak current (E_{1ox}) and the scan rate is observed in the inset of Figure 3 for poly(**2**) and poly(**3**) with a correlation factor $R > 0.999$. This linear fit confirms that charge transport through the film is not diffusion limited as well as the stability to p-doping.[42,45]

Thermogravimetric Analysis of Poly(2) and Poly(3). Thermogravimetric analysis (TGA) of poly(**2**) and poly(**3**) was performed under dynamic N_2 atmosphere. For comparison, TGA experiments were also performed for electrochemically synthesized PEDOT and poly(pyrrole) (PPy).

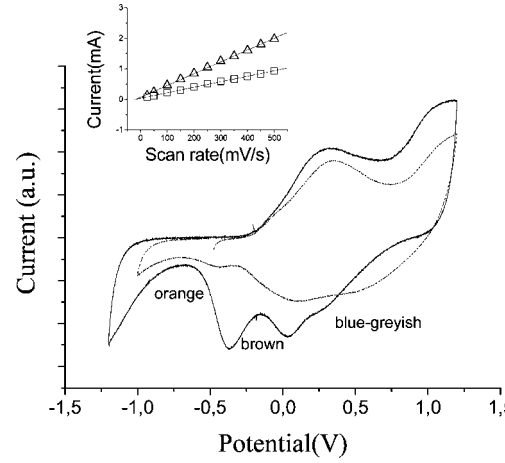

Figure 3. Cyclic voltammogram of poly(**2**) (dashed line) and poly(**3**) (solid line) using indium tin oxide (ITO) plastic sheet as working electrode, Ag/AgCl as reference electrode, Pt sheet as counter electrode and 0.1 M $LiClO_4$ in acetonitrile at a scan rate of 100 mV s^{-1}. Inset: Plot of scan rate (mV/s) vs current (mA) for poly(**2**) (□) and poly(**3**) (△) in a monomer free solution.

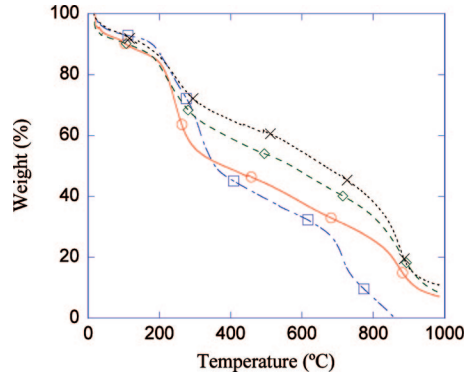

Figure 4. High-resolution TGA of PPy (○), PEDOT (□), poly(**2**) (◇) and poly(**3**) (×) under nitrogen atmosphere. Heating rate: 10 °C/min from 20 to 1000 °C.

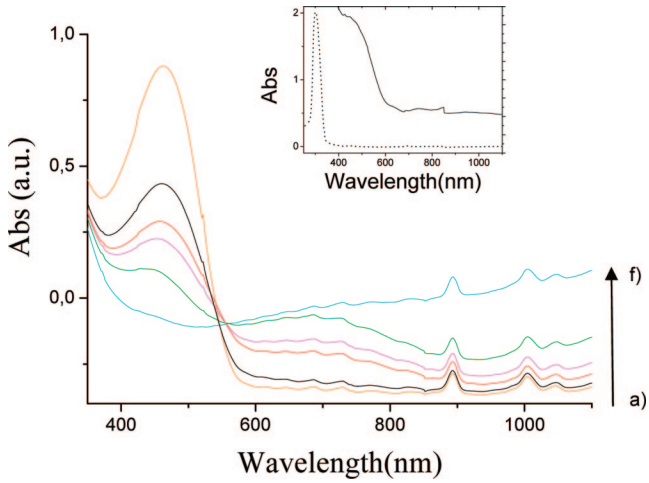

Figure 5. UV/vis/NIR spectroelectrochemistry for poly(**2**) on indium tin oxide (ITO) plastic; Pt wire counter electrode, Ag/AgCl reference electrode, $LiClO_4$ supporting electrolyte (0.1 M): (a) −0.8 V; (b) −0.2 V; (c) −0.1 V; (d) 0 V; (e) 0.2 V; (f) 0.8 V. Inset: Absorption spectra for poly(**2**) dedoped (solid line) and monomer **2** in acetonitrile (dashed line).

Figure 4 displays the high-resolution TGA curves of the different polymers at a heating rate of 10 °C/min, from room temperature to 1000 °C.

An initial weight loss is observed for all the polymers between room temperature and about 150−170 °C, that can be assigned to the loss of variable amounts of solvent or water loosely bonded to the polymer chains.[46] The percentage assigned to the solvent/water loss is in the range of 4−8%.

The polymers were stable up to 200 °C where the first significant weight loss was observed. This weight loss can be tentatively attributed to the lack of dopant as it is explained in similar research work based on conducting polymers.[47,48] After the dopant loss step, all the polymers show a constant decrease of weight due to the degradation of the polymer backbone. The residue of the different polymers at 800 °C was 34% for poly(**2**), 39% for poly(**3**), 7% for PEDOT, and 19% for PPy.

Spectroelectrochemical and Electrochromic Properties of Poly(2) and Poly(3) Films. The absorption spectrum of monomer **2**, together with that of the corresponding polymer, is represented in Figure 5, inset. The absorption maxima in the UV/vis/NIR spectra of monomers **2** and **3** were similar (302−303 nm in acetonitrile) and close to that of monomer **1** (306 nm in dichloromethane). The electrochemically deposited polymers, poly(**2**) and poly(**3**), on ITO plastic as-grown exhibited a λ_{max} in the range of 459−463 nm and a weak peak

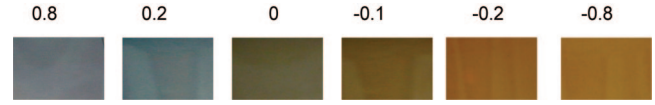

Figure 6. Multichromic behavior of poly(**3**) at +0.8 V (blue-grayish), +0.2 V (light blue), 0 V (light brown), −0.1 V (brown), −0.2 V (dark orange), and −0.8 V (light orange).

centered at 708−715 nm arising from the doped state of the polymers. These films were fully dedoped for 1 h, and the corresponding UV/vis/NIR spectra were recorded showing no sign of the second band corresponding to the polaron charge carriers.

The difference between the λ_{max} corresponding to the monomer and the corresponding polymer for derivatives **2** and **3**, which is higher than 100 nm, is indicative of increased conjugation length in the polymer. This is a typical trend in conducting polymers.[16]

Spectroelectrochemical study of poly(**2**) and poly(**3**) was carried out by varying the voltage with 0.1 V steps between +1.0 and −0.8 V. In order to perform the experiment, an optical transparent electrode cell was employed using a traditional 3 electrode setup. Therefore, the corresponding polymer was deposited on ITO plastic to study the changes in the optical properties upon application of different potentials. Both polymers revealed multicolor electrochromism exhibiting several colored states: orange-yellowish, dark orange, brown, blue and blue-grayish upon oxidation, showing both cathodic and anodic coloring electrochromism (Figure 6). An in-depth colorimetry study is reported in the next section.

Figure 5 depicts the different profiles observed at each potential (−0.8, −0.2, −0.1, 0, +0.2 and +0.8 V) which are related with the range of colors obtained. The absorption maximum for poly(**2**) in the reduced state at −0.8 V was found to be 464 nm corresponding to the $\pi \rightarrow \pi^*$ transition. Upon oxidation, the intensity of the $\pi \rightarrow \pi^*$ transition decreases while the polaron broad absorption band at longer wavelength (centered at 700 nm) increases in intensity. This band emerges at −0.1 V and increases in intensity up to +0.2 V. From +0.2 V to +0.8 V, it presented no significant changes. However, the band at 464 nm disappears upon further oxidation at +0.8 V. An isosbestic point is observed at 548 nm. Very similar behavior is observed for poly(**3**), so no further information is given.

The as-grown polymers exhibit a blue-grayish color, and each film is evaluated from +1 to −0.9 V in order to study the range of colors in a wider interval of potentials. At +0.8 V both polymers exhibit the blue-grayish color which passes to a light blue color at +0.2 V. The polymer turns into a brown intermediate state at 0 V before obtaining a dark orange reduced state at −0.2 V, to finish in an orange-yellowish color at −0.8 V. Although both polymers presented multichromism, poly(**3**) presented brighter colors in comparison to poly(**2**) for polymeric films of similar thickness (∼100 nm). These different colors have also been corroborated with the cyclic voltammetry of the corresponding polymeric films (see Figure 3). This multicolor property from a single material may have significant implications for device applications since several colors are desirable from a single electroactive material.

The optical contrast of poly(**2**) and poly(**3**) was determined for different polymer thicknesses in order to obtain the optimum thickness which will lead to the maximum optical contrast. The contrast is given as the transmittance difference between the reduced and oxidized states and is reported as ΔT %. Figure 7 shows the evolution of the optical contrast vs film thickness.

The optical contrast (ΔT %) varies from ∼22% to 29.5% for poly(**2**). After 2 electrodepositing scans (corresponding to a film thickness of ∼14 nm), poly(**2**) presented an optical contrast

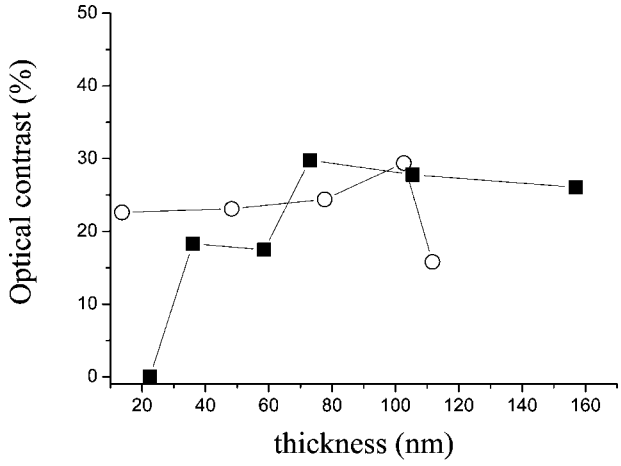

Figure 7. Plot of optical contrast (ΔT %) vs film thickness (nm) for poly(**2**) (○) and poly(**3**) (■).

higher than 22%. This value was practically constant at 4 and 6 scans (48 and 78 nm, respectively), giving the maximum optical contrast at 8 cycles (102 nm) and finally decreasing after 10 cycles (112 nm). Surprisingly, poly(**3**) showed negligible optical contrast for a film prepared at 2 electrodepositing scans (22 nm), while a polymeric film prepared at 4 scans (36 nm) gave an optical contrast of 18.4%. The optical contrast observed for poly(**3**) varies from 18 to 30%. It is noteworthy that both polymers presented the maximum optical contrast (ΔT % = 30%) for a polymeric film prepared electrochemically after 8 electrodepositing scans. As a reference, the unsubstituted polymer poly(**1**) presented a maximum optical contrast of 35% after 6 electrodepositing cycles.[16]

The coloration efficiency defined as the change in optical density per charge passed through the film during the bleaching process was 107 cm^2/C for poly(**2**) and 108 cm^2/C for poly(**3**) (surface area employed in the measurements: 0.75 cm^2). For comparison, poly(bithiophene) electrochemically prepared on ITO glass exhibited a coloration efficiency of 110 cm^2/C[49] and PEDOT 183 cm^2/C.[50]

In order to study the kinetics of the electrochromic behavior of poly(**2**) and poly(**3**), the polymers were switched by repeated potential steps between their oxidized (+1 V) and reduced (−0.9 V) states. In these studies, the optical contrast of the polymer film was monitored as a function of time at the wavelength corresponding to the maximum optical contrast (464 nm). Quantification of switching time was performed by defining a change in 90% of the total absorbance span (Figure 8). The optical response in poly(**2**) was 2 s for the oxidation process (blue-grayish) and 4 s for the reduction process (orange-yellowish) while poly(**3**) needed 3 s to be oxidized (blue-grayish) and it was reduced in only 1 s (orange-yellowish).

Poly(**3**) showed a faster bleaching process in comparison with the coloring process, which means a faster kinetics of dopant ion diffusion in the reduction process than for the reverse process. On the other hand, poly(**2**) showed a faster coloring process, due to faster kinetics of dopant ion diffusion in the oxidation process. However, both polymers present fast switching time in the range of a few seconds, and the slight discrepancy in the time required to achieve 90% of the coloring and decoloring states may be due to the conditions of electrodeposition and the resulting thickness of the polymeric films.

Colorimetry Study of Poly(2) and Poly(3). The colors of poly(**2**) and poly(**3**) were determined by performing colorimetry measurements. CIE 1976 L*a*b* color spaces and CIE 1931 Yxy recommended by the commission internationale de l'Eclairage (CIE)[51] were used as the quantitative scale to define

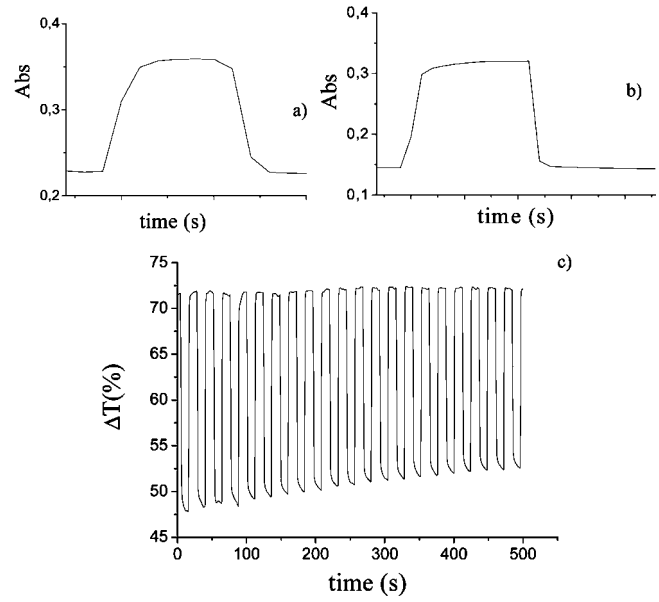

Figure 8. Optical switching studies for poly(**2**) (a) and poly(**3**) (b and c) films monitored at 464 nm in 0.1 M $LiClO_4$/acetonitrile.

Table 1. CIE xy and L*a*b* Color Spaces for Poly(2) and Poly(3) as a Function of Applied Potential

polymer	potential (V)	L^*	a^*	b^*	x	y
poly(**2**)	1	27.57	−1.58	0.80	0.3312	0.3397
	0.8	23.07	3.70	−5.97	0.3179	0.2978
	0.2	27.98	−7.80	−0.81	0.3025	0.3432
	0	34.26	3.67	14.54	0.4002	0.3805
	−0.1	33.28	9.79	15.11	0.4239	0.3703
	−0.2	31.91	13.57	25.21	0.4754	0.3928
	−0.8	35.94	7.45	21.16	0.4329	0.3924
poly(**3**)	1	32.4	−4.75	−1.1	0.3139	0.3363
	0.9	35.2	−5.78	8.45	0.3468	0.3755
	0	32.8	1.5	10.9	0.381	0.373
	−0.1	33.6	4.85	23.7	0.4372	0.4087
	−0.3	43.4	7.73	42.5	0.4769	0.4362
	−0.5	40.6	16.4	34.3	0.4885	0.4018

the colors. The attributes of color, hue (a), saturation (b) and luminance (L), were measured in situ at the oxidized, intermediate and reduced states in addition to states in between, and the results are summarized in Table 1.

Colorimetry measurements for poly(**2**) and poly(**3**) were taken every 100 mV in the active range (+1 to −0.9 V). In electrochromic polymers, the L*a*b* data are normally accomplished by recording the Yxy color space coordinates at different potentials. The data obtained are often plotted using CIE 1931 color coordinates to visually depict the path of the material's color change during potential switching. Figure 9 depicts the CIE color space plots for poly(**2**) (results for poly(**3**) were very similar so they are not shown).

The color corresponding to the oxidized state is located in the light blue region. As the polymer is reduced, it moves to the brown and orange regions. Very similar results were obtained for poly(**3**).

Morphology of Poly(2) and Poly(3) Films by AFM. Thin films of poly (**2**) (∼14 nm) and poly(**3**) (∼22 nm) showed, as prepared, a roughness mean square (rms) of 4.4 and 2.2 nm, respectively, as determined by profilometry.

Films electrodeposited on ITO plastic corresponding to poly(**2**) and poly(**3**) were studied by AFM using the same conditions previously employed for poly(**1**).[16] Since poly(**2**) and poly(**3**) presented multichromic behavior as a function of potential, the polymeric films were studied at three different

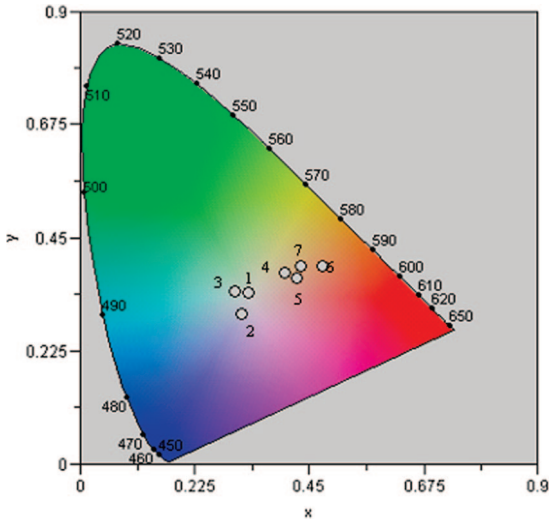

Figure 9. CIE chromaticity diagram showing the (*x*,*y*) color coordinates of poly(**2**) films deposited on ITO. The numbers in the graph correspond to 1 (as grown, blue-grayish), 2 (+1 V, blue-grayish), 3 (+0.8 V, light blue), 4 (0 V, light brown), 5 (−0.1 V, brown), 6 (−0.2 V, dark orange) and 7 (−0.8 V, light orange).

potentials: +1 V (blue-grayish), 0 V (light brown) and −0.5 V (dark orange).

Figure 10 displays the 3D and 2D AFM topography images for both polymers in the oxidized, neutral and reduced states. Both polymers presented different morphologies at each redox state (oxidized, neutral and reduced state). When comparing poly(**2**) and poly(**3**) to each other at the same redox state, the morphology is quite different.

The main conclusions obtained from the AFM measurements are as follows: (1) poly(**2**) presented a much rougher surface in comparison to poly(**3**); (2) the morphology for both polymers in the oxidized state (+1 V) is sharp; (3) upon reduction, the polymer's surface was smooth. Surprisingly, the morphology evolution of poly(**2**) and poly(**3**) films is different from that reported previously for poly(**1**). [16] The potential influence of stereochemistry (conformations) on the observed morphology is investigated in next section.

Quantum Chemical Calculations of 2-(2-Thienyl)-1*H*-pyrrole Derivatives. In view of the remarkable difference in the morphologies and the electrochromic behavior of poly(**2**) and poly(**3**) when compared to those observed for poly(**1**), vide supra, it was justified and highly desirable to examine the influence of the alkyl substituents in the pyrrole ring on the stereochemistry (conformations), charge distribution and ionization potentials of monomers **1**−**3**. To reach these goals, we have employed high-level ab initio calculations. Complementary to the title compounds, three other members from this series, namely, 3-methyl-, 3-*i*-propyl- and 3-*t*-butyl-2-(2-thienyl)-1*H*-pyrrole, were also investigated. Geometry optimizations, theoretical conformational analysis and calculation of Mulliken charges were performed at the B3LYP/6-311G* level, while ionization potentials were calculated as the energy differences between the neutral molecules and the related radical cations at the MP2/6-311G** level of theory (Table 2).

The monomer derivatives under study consist of two moieties having different electron-releasing ability, i.e. they should demonstrate two different ionization energies as well as two different oxidation potentials. Therefore, a stepwise ionization and electrochemical oxidation are expected to be observed for each monomer. For pyrrole, experimental (8.3 eV)[52] and calculated (8.10, 7.89, 8.09 eV by HF, OVGF and ADC(3), respectively)[53] values of ionization potential indicate that ionization potentials calculated in this work correspond to the ionization of the pyrrole moiety of the monomers (Table 2). At the same time, for thiophene the experimental (9.0 eV) and calculated values of ionization potentials imply that the ionization of the thiophene moiety of the monomers will occur at around 9 eV, being actually the second ionization potential. Consequently, the first oxidation process (E_{1ox} = +0.84 V for **2** and +0.80 V for **3**) relates to the oxidation of pyrrole moieties to deliver the radical cation A, which then further recombines to dimer B (Scheme 4). Although there are two competitive reaction pathways in the electropolymerization of thiophene and pyrrole (through α and β positions), the reactivity of the α and β positions is about 95/5, which is in good agreement with the proposed structure of the dimer.[44]

It is noteworthy that for all compounds under study except for 3-*t*-butyl-2-(2-thienyl)-1*H*-pyrrole two conformers, skewed *s-cis* and skewed *s-trans*, both with considerable out-of-plane deviations, were localized on the rotational potential energy surface, as illustrated below for the parent member of this series, 2-(2-thienyl)-1H-pyrrole, **1**:

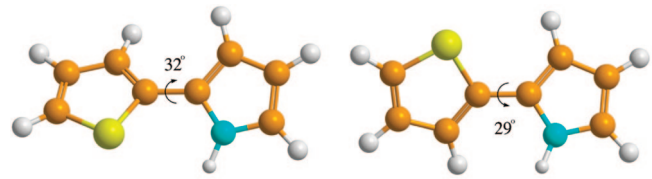

Apparently, there is a notable difference in the conformational behavior of **2** and **3** as compared to **1**, resulting in an increased population of the *s-cis* conformer in the former two compounds. On the other hand, the non-coplanarity of the rings (out-of-plane deviations, φ) is increased in **2** and **3** as compared to **1**, and these both trends are even more pronounced in 3-*t*-butyl-2-(2-thienyl)-1*H*-pyrrole having the most bulky alkyl substituent at position 3 of the pyrrole ring.

For the latter, only one orthogonal conformer with the dramatic out-of-plane deviation of $\varphi = 83°$ has been localized and, as a result, the Mulliken charges were more negative on nitrogen and more positive on sulfur in this compound, relative to other members of this series, which is due to the decreased π,π-conjugation between the pyrrole (π-donor) and the thiophene (π-acceptor) rings, see Table 2. However, the vertical ionization potential of 3-*t*-butyl-2-(2-thienyl)-1*H*-pyrrole is only slightly increased with respect to other compounds.

Present theoretical results are in line with the early conformational study of unsubstituted 2-(2-thienyl)-1*H*-pyrrole.[54] The latter was shown to exist as the equilibrium mixture of *s-cis* and *s-trans* conformers, both with the considerable out-of-plane deviations, separated by a barrier of ca. 1.5 kcal/mol, as follows from the HF, MP2 and B3LYP calculations with small basis set.

From the present computational results, even a more clear-cut electrochromic behavior for poly(3-*t*-butyl-2-(2-thienyl)-1*H*-pyrrole) as well as for polymers with longer-chain substituents at the position 3 could be expected. Experiments are currently under way to confirm these theoretical predictions.

Taking into account the predominant conformations of starting monomers **2** and **3** it is conceivable that the resulting polymers poly(**2**) and poly(**3**) will have the chain conformations with preferred *s-cis* disposition of the sulfur and nitrogen atoms, which is due to the unfavorable steric interactions of alkyl groups with the diffuse hybridized sulfur lone pair in the minor *s-trans* conformations of poly(**2**) and poly(**3**) as compared to poly(**1**).

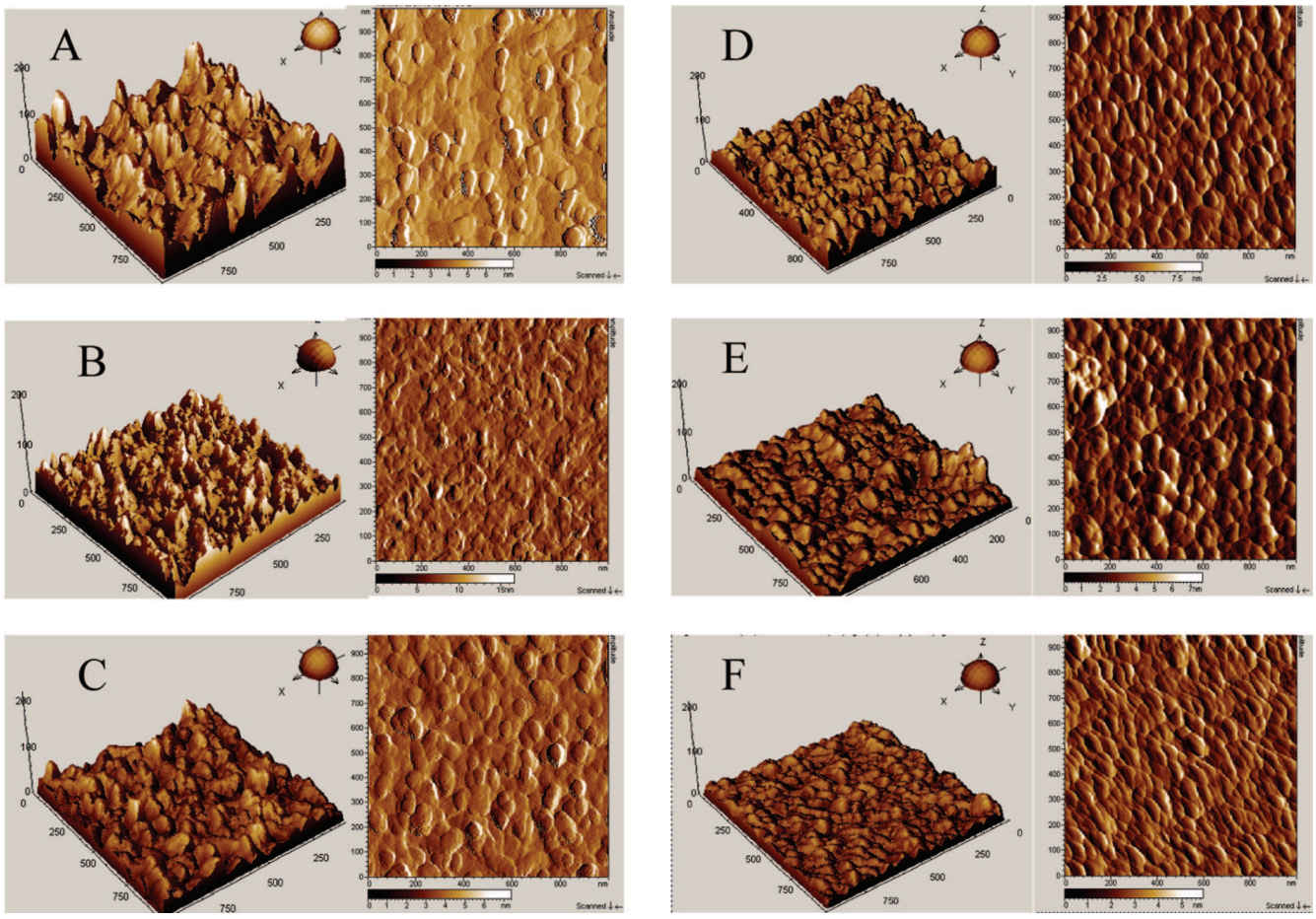

Figure 10. AFM morphology for poly(**2**) at +1 V (A), 0 V (B) and −0.5 V (C) in 3D (left) and 2D (right) images and for poly(**3**) at +1 V (D), 0 V (E) and −0.5 V (F) in 3D (left) and 2D (right) images.

Table 2. Results of the Quantum Chemical Calculations of 3-Alkyl-2-(2-thienyl)-1*H*-pyrroles

alk	conformer	mole fraction (%)	out-of-plane deviation φ (deg)	Mulliken charges (eu) q_N	Mulliken charges (eu) q_S	vertical ionization potential I (eV)
H	*s-cis*	49	32	−0.70	0.23	8.02
	s-trans	51	29	−0.70	0.25	7.99
Me	*s-cis*	72	34	−0.71	0.23	7.92
	s-trans	28	34	−0.71	0.27	7.88
Et	*s-cis*	69	38	−0.71	0.23	7.96
	s-trans	31	41	−0.70	0.28	7.95
n-Pr	*s-cis*	65	46	−0.70	0.24	8.01
	s-trans	35	47	−0.69	0.27	7.98
i-Pr	*s-cis*	69	42	−0.71	0.23	7.99
	s-trans	31	46	−0.70	0.27	7.98
t-Bu	*orthogonal*	100	83	−0.76	0.33	8.13

Scheme 4

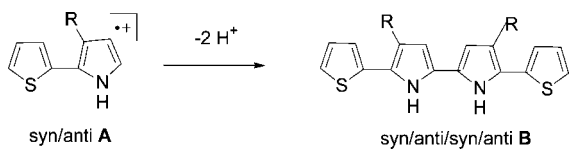

syn/anti **A** syn/anti/syn/anti **B**

Conclusions

A new multichromic polymeric series resulting from electropolymerization of 3-alkyl-2-(2-thienyl)-1*H*-pyrrole derivatives has been described. Contrary to poly(2-(2-thienyl)-1*H*-pyrrole), poly(**1**), showing dual orange-to-black electrochromic behavior, poly(3-ethyl-2-(2-thienyl)-1*H*-pyrrole), poly(**2**), and poly(3-*n*-propyl- 2-(2-thienyl)-1*H*-pyrrole), poly(**3**), showed multicolor electrochromism (both cathodic and anodic) exhibiting several colored states: blue-grayish (+0.8 V), light blue (+0.2 V), light brown (0 V), brown (−0.1 V), dark orange (−0.2 V) and light orange (−0.8 V).

These new electroactive polymers have been thoroughly characterized by spectroelectrochemical, thermogravimetric, colorimetric and atomic force microscopy techniques. Quantum chemical calculations were performed to examine the influence of the alkyl substituents on the stereochemistry (conformations), charge distribution and ionization potentials of 3-alkyl-2-(2-thienyl)-1*H*-pyrrole derivatives. Based on such calculations, interesting electrochromic behavior is expected for poly(3-*t*-butyl-2-(2-thienyl)-1*H*-pyrrole). Experiments are in progress to confirm this theoretical prediction.

Experimental Section

General. All starting chemicals were purchased from Aldrich Chemical and used without further purification. Pyrrole was distilled before use. NMR spectra were recorded on a Bruker DPX 400 spectrometer (400.13 MHz, ^{1}H; 101.61 MHz, ^{13}C) with HMDS as an internal standard. IR spectra were obtained on a Bruker IFS 25 instrument. UV/visible measurements were carried out in a Jasco V-570 spectrophotometer. The electrochemical characterization was performed in a typical three electrode set-up using an EC-Laboratory MPG Biologic multipotentiostat employing both Pt sheet and ITO as working electrodes, Pt sheet as counter electrode and Ag/AgCl as reference electrode. The experiments were carried out in 10^{-3} M monomer solution in acetonitrile and 0.1 M $LiClO_4$ acetonitrile solution as supporting electrolyte. Electrochemical films from precursors **2** and **3** were obtained after successive scanning over the first oxidation process

leading to a thin film which switches from blue-gray to yellow-orange film upon reduction.

AFM images of the films were obtained with a Molecular Imaging "PicoPlus" atomic force microscope operating in acoustic mode for the solution side of thin films of poly(**2**) and poly(**3**) on ITO substrate, in both the oxidized and reduced states. Colorimetry was carried out with a Minolta CS1000 spectroradiometer. The thickness and roughness (rms) of the films were determined using an Ambios XP1 profilometer. Thermogravimetric experiments were performed on a High-Res TGA Q500.

Becke's three-parameter hybrid functional[55] (where nonlocal correlation is provided by Lee, Yang and Parr correlation functional[56]) and MP2 (second-order perturbation theory of Møller and Plesset) levels using the 6-311G* and 6-311G** basis sets of Pople and co-workers[57] with GAMESS code[58] compiled on Quantum chemical calculations were performed at the DFT-B3LYP (density functional theory using LINUX (Kernel 2.6.16) platform).

Synthesis of Monomer 2 from 1-(2-Thienyl)-1-butanone Oxime and Acetylene. 1-(2-Thienyl)-1-butanone oxime (5.0 g, 29.5 mmol) and KOH·0.5H_2O (1.92 g, 29.5 mmol) were dissolved under heating (90−95 °C) in DMSO (75 mL). The solution of potassium oximate thus obtained was placed into a 0.25−l steel rotating autoclave. Then acetylene was released to remove air and the autoclave was charged with acetylene again from a cylinder at room temperature (initial pressure: 14 atm). The autoclave was heated upon rotating (95−100 °C) for 20 min (acetylene pressure reached its maximum: 20−25 atm, and the pressure dropped rapidly due to the reaction of acetylene with ketoxime). The reaction mixture, after cooling to room temperature, was diluted with a 3-fold volume excess of ice water and extracted with diethyl ether (5 mL × 5). The ether extracts were washed with cold water (5 mL × 3) to remove dissolved DMSO. Then the mixture was dried over K_2CO_3 overnight, ether was removed and the residue (5.01 g) was analyzed by ^{1}H NMR. Crude product contained (^{1}H NMR) 68% of 3-ethyl-2-(2-thienyl)-1*H*-pyrrole **2** and 32% of 3-ethyl-2-(2-thienyl)-1-vinylpyrrole **4**. For isolation of pure **2** column chromatography (basic Al_2O_3) was applied. First, **4** was eluted with hexane, and then, **2** was eluted with the system hexane−ether (20:1). After evaporation of solvents, 1.95 g (37% yield) of pure **2** was obtained as a viscous green liquid, n_D^{20} 1.6681 (literature 1.6675[29]). Found %: C 67.91, H 6.22, N 7.83, S 18.20. Calcd % for $C_{10}H_{11}NS$: C 67.76, H 6.25, N 7.90, S 18.09. ^{1}H NMR (δ, $CDCl_3$): 8.02 (1H, br s, NH), 7.14 (1H, dd, H-5′, $^3J_{4'-5'}$ 4.9 Hz, $^4J_{3'-5'}$ 0.9 Hz), 6.99 (1H, m, H-3′), 6.91 (1H, m, H-4′), 6.65 (1H, m, H-5), 6.14 (1H, m, H-4), 2.64 (2H, q, $^3J_{CH2-CH3}$). ^{13}C NMR (δ, $CDCl_3$): 135.7 (C-2′), 127.3 (C-4′), 123.9 (C-2), 123.0 (C-5′), 122.2 (C-3′), 122.0 (C-3), 117.6 (C-5), 109.9 (C-4), 19.6 (CH_2), 15.1 (Me). IR (film, cm^{-1}): 3416 (NH), 1525, 1036, 696 (thiophene ring), 1578, 1511, 1375, 696 (pyrrole ring). UV/vis (MeCN): λ_{max} 304 nm, lg ε 4.06.

One-Pot Synthesis of Monomer 2 from 1-(2-Thienyl)-1-butanone, Hydroxylamine and Acetylene. Hydroxylamine hydrochloride (0.90 g, 13 mmol) was dissolved in DMSO (50 mL) in a 100 mL flask equipped with a magnetic stirrer, and then $NaHCO_3$ (1.09 g, 13 mmol) and 1-(2-thienyl)-1-butanone (2.00 g, 13 mmol) were added upon vigorous stirring. The intense evolution of CO_2 was observed. The mixture was allowed to stand for 2 h at 70−80 °C until the reaction completed and the remaining CO_2 was blown out with a nitrogen flow. Then the mixture was placed into a 0.25 L steel rotating autoclave, the KOH·0.5H_2O (0.85 g, 13 mmol) was added and acetylene was fed from a cylinder at room temperature (initial pressure: 14 atm). The autoclave was heated (95−100 °C) for 30 min (acetylene pressure reached its maximum 20−25 atm, then the pressure dropped rapidly due to the reaction of acetylene with ketoxime). The reaction mixture, after cooling to room temperature, was diluted with a 3-fold volume excess of ice water, neutralized with CO_2 (gas) and extracted with dichloromethane (5 mL × 5). The dichloromethane extracts were washed with water (5 mL × 3) to remove dissolved DMSO, then the mixture was dried over K_2CO_3 overnight, dichloromethane was removed and the residue (1.91 g) was analyzed by GLC or ^{1}H NMR. Crude product contained (^{1}H NMR) 72% of 3-ethyl-2-(2-thienyl)-1*H*-pyrrole **2**, 14% of 3-ethyl-2-(2-thienyl)-1-vinylpyrrole **4** and 14% of 1-(2-thienyl)-1-butanone O-vinyloxime **6**. For isolation of pure **2** column chromatography (basic Al_2O_3) was applied. First, **4** and **6** were eluted with hexane, and then, **2** was eluted with the system hexane−ether (20:1). After evaporation of eluents 1.07 g (47% yield) of **2** was obtained.

Synthesis of Monomer 3 from 1-(2-Thienyl)-1-pentanone Oxime and Acetylene. 1-(2-Thienyl)-1-pentanone oxime (5.0 g, 27.3 mmol) and KOH·0.5H_2O (1.77 g, 27.3 mmol) were dissolved under heating (90−95 °C) in DMSO (75 mL). The solution of potassium oximate thus obtained was placed into a 0.25 L steel rotating autoclave and acetylene was fed from a cylinder at room temperature (initial pressure: 14 atm). The autoclave was heated (95−100 °C) for 5 min. The reaction mixture, after cooling to room temperature, was diluted with a 3-fold volume excess of ice water, neutralized with CO_2 (gas) and extracted with diethyl ether (5 mL × 5). The ether extracts were washed with cold water (5 mL × 3) to remove dissolved DMSO, then the mixture was dried over K_2CO_3 overnight, the ether was removed and the residue (4.83 g) was analyzed by ^{1}H NMR. Crude product contained (^{1}H NMR) 77% of 3-*n*-propyl-2-(2-thienyl)-1*H*-pyrrole **3** and 23% of 3-propyl-2-(2-thienyl)-1-vinylpyrrole **5**. For isolation of pure **3** column chromatography (basic Al_2O_3) was used. First, **5** was eluted with hexane, and then, **3** was eluted with the system hexane−ether (20:1). After evaporation of solvents 2.26 g (43% yield) of pure **3** was obtained as a red viscous liquid, n_D^{20} 1.6310. Found %: C 69.27, H 6.72, N 7.43, S 17.00. Calcd % for $C_{11}H_{13}NS$: C 69.07, H 6.85, N 7.32, S 16.76. ^{1}H NMR (δ, $CDCl_3$): 8.09 (1H, br s, NH), 7.18 (1H, dd, H-5′, $^3J_{4'-5'}$ 4.7 Hz, $^4J_{3'-5'}$ 0.9 Hz), 7.02 (1H, m, H-3′), 6.98 (1H, m, H-4′), 6.73 (1H, m, H-5), 6.15 (1H, m, H-4). ^{13}C NMR (δ, $CDCl_3$): 135.9 (C-2′), 127.4 (C-4′), 123.2 (C-2), 122.6 (C-5′), 122.4 (C-3′), 119.6 (C-3), 117.6 (C-5), 110.7 (C-4), 28.8 (CH_2), 24.2 (CH_2), 14.2 (Me). IR (film, cm^{-1}): 3414 (NH), 1525, 1041, 693 (thiophene ring), 1579, 1511, 1378, 693 (pyrrole ring). UV/vis (MeCN): λ_{max} 304 nm, lg ε 3.96.

Acknowledgment. The authors thank Eider Beguiristain for excellent technical assistance. C.P.-G. thanks the Spanish Ministry of Education and Science (Grant No. MAT2006-13894-C03-01) and CIC Nanogune−Consolider (Grant No. CSD2006-53).

References and Notes

(1) Kirchmeyer, S.; Reuter, K. *J. Mater. Chem.* **2005**, *15*, 2077–2088.
(2) Gaupp, C. L.; Reynolds, J. R. *Macromolecules* **2003**, *36*, 6305–6315.
(3) Sapp, S. A.; Sotzing, G. A.; Reynolds, J. R. *Chem. Mater.* **1998**, *10*, 2101–2108.
(4) Niklasson, G. A.; Granqvist, C. G. *J. Mater. Chem.* **2007**, *17*, 127–156.
(5) Mortimor, R. J.; Dyer, A. L.; Reynolds, J. R. *Displays* **2006**, *27*, 2–18.
(6) Dyer, A. L.; Grenier, C. R. G.; Reynolds, J. R. *Adv. Funct. Mater.* **2007**, *17*, 1480–1486.
(7) Pozo-Gonzalo, C.; Mecerreyes, D.; Pomposo, J. A.; Salsamendi, M.; Marcilla, R.; Grande, H.; Vergaz, R.; Barrios, D.; Sánchez-Pena, J. *Sol. Energy Mater. Sol. Cells* **2008**, *92*, 101–106.
(8) Wang, X. J.; Lau, W. M.; Wong, K. Y. *Appl. Phys. Lett.* **2005**, *87*, 113502.
(9) Mortimer, R. J. *Chem. Soc. Rev.* **1997**, *26*, 147–156.
(10) Liu, G.; Richardson, T. J. *Sol. Energy Mater. Sol. Cells* **2005**, *86*, 113–121.
(11) Varis, S.; Ak, M.; Akhmedov, I. M.; Tanyeli, C.; Toppare, L. *J. Electroanal. Chem.* **2007**, *603*, 8–14.
(12) DuBois, C. J.; Reynolds, J. R. *Adv. Mater.* **2002**, *14*, 1844–1846.
(13) Argun, A. A.; Aubert, P. H.; Thompson, B. C.; Schwendeman, I.; Gaupp, C. L.; Hwang, J.; Pinto, N. J.; Tanner, D. B.; MacDiarmid, A. G.; Reynolds, J. R. *Chem. Mater.* **2004**, *16*, 4401–4412.
(14) Kraft, A.; Rottman, M.; Gilsing, H. D.; Faltz, H. *Electrochim. Acta* **2007**, *52*, 5856–5862.
(15) Song, H. K.; Lee, E. J.; Oh, S. M. *Chem. Mater.* **2005**, *17*, 2232–2233.
(16) Pozo-Gonzalo, C.; Pomposo, J. A.; Alduncin, J. A.; Salsamendi, M.; Mikhaleva, A. I.; Krivdin, L. B.; Trofimov, B. A. *Electrochim. Acta* **2007**, *52*, 4784–4791.
(17) Naitoh, S. *Synth. Met.* **1987**, *18*, 237–240.

(18) Ping, Z.; Federspiel, P.; Grünberger, A.; Nauer, G. E. *Synth. Met.* **1997**, *84*, 837–838.
(19) Naitoh, S.; Sanui, K.; Ogata, N. *J. Chem. Soc., Chem. Commun.* **1986**, 1348–1349.
(20) Ping, Z.; Federspiel, P.; Grünberger, A.; Nauer, G. E. *Synth. Met.* **1997**, *84*, 837–838.
(21) Ping, Z.; Nauer, G. E. *Synth. Met.* **1997**, *84*, 577–578.
(22) Ping, Z.; Nauer, G. E. *Synth. Met.* **1997**, *84*, 843–844.
(23) Trofimov, B. A.; Mikhaleva, A. I.; Nesterenko, R. N.; Vasil'ev, A. N.; Nakhmanovich, A. S.; Voronkov, M. G. *Khim. Geterotsikl. Soedin.* **1977**, *8*, 1136–1137.
(24) Pozo-Gonzalo, C.; Khan, T.; McDouall, J. J. W.; Skabara, P. J.; Roberts, D. M.; Light, M. E.; Coles, S. J.; Hursthouse, M. B.; Neugebauer, H.; Cravino, A.; Sariciftci, N. S. *J. Mater. Chem.* **2002**, *12*, 500.
(25) Trofimov, B. A. In *Adv. Heterocycl. Chem.*; Katritzky, A. R., Ed.; Acad. Press: San Diego, 1990; Vol. *51*, p 177.
(26) Bean, G. P. In *The Chemistry of Heterocyclic Compounds. Pyrroles, Part 2*; Jones, R. A., Ed.; Wiley: New York, 1992; Vol. *48*, p 105.
(27) Tedeschi, R. J. In *Encyclopedia of Physical Science and Technology*; Acad. Press: San Diego, 1992; Vol. *1*, p 27.
(28) Mikhaleva, A. I.; Yu.Schmidt, E. In *Selected methods for synthesis and modification of heterocycles*; Kartsev, V. G., Ed.; IBS Press: Moscow, 2002; Vol. *1*, p 334.
(29) Trofimov, B. A.; Mikhaleva, A. I.; Nesterenko, R. N.; Vasiliev, A. N.; Nakhmanovich, A. S.; Voronkov, M. G. *Khim. Geterotsikl. Soed.* **1977**, 1136–1139.
(30) Korostova, S. E.; Mikhaleva, A. I.; Nesterenko, R. N.; Maznaya, N. V.; Voronov, V. K.; Borodina, N. M. *Zh. Org. Khim.* **1985**, *21*, 406–411.
(31) Korostova, S. E.; Nesterenko, R. N.; Mikhaleva, A. I.; Polovnikova, R. I.; Golovanova, N. I. *Khim. Geterotsikl. Soedin.* **1989**, *63*, 901–906.
(32) Yu. Schmidt, E.; Mikhaleva, A. I.; Vasil'tsov, A. M.; Zaitsev, A. B.; Zorina, N. V. *Arkivoc* **2005**, 11–17.
(33) Mikhaleva, A. I.; Yu. Schmidt, E.; Ivanov, A. V.; Vasil'tsov, A. M.; Yu. Senotrusova, E.; Protsuk, N. I. *Zh. Org. Khim.* **2007**, *43*, 236–298.
(34) Reeves, B. D.; Grenier, C. R. G.; Argun, A. A.; Cirpan, A.; McCarley, T. D.; Reynolds, J. R. *Macromolecules* **2004**, *37*, 7559–7569.
(35) Groenendaal, L. B.; Zotti, G.; Auber, P. H.; Waybright, S. M.; Reynolds, J. R. *Adv. Mater.* **2003**, *15*, 855–879.
(36) Sankaran, B.; Reynolds, J. R. *Macromolecules* **1997**, *30*, 2582–2588.
(37) Arbizzani, C.; Mastragostino, M.; Nevi, L.; Rambelli, L. *Electrochim. Acta* **2007**, *52*, 3274–3279.
(38) Conwell, E. M. In *Handbook of organic conductive molecules and polymers*; Nalwa, H. S., Ed.; Wiley: New York, 1997; Vol. *4*, p 1.
(39) Menon, V. P.; Lei, J.; Martin, C. R. *Chem. Mater.* **1996**, *8*, 2382–2390.
(40) Han, M. G.; and Foulger, S. H. *Small* **2006**, *2*, 1164–1169.
(41) Zotti, G.; Zecchin, S.; Schiavon, G.; Louwet, F.; Groenendaal, L.; Crispin, X.; Osikowicz, W.; Salaneck, W.; Fahlman, M. *Macromolecules* **2003**, *36*, 3337–3344.
(42) Pozo-Gonzalo, C.; Khan, T.; Mc. Douall, J. J. W.; Skabara, P. J.; Roberts, D. M.; Light, M. E.; Coles, S. J.; Hursthouse, M. B.; Neugebauer, H.; Cravino, A.; Sariciftci, N. S. *J. Mater. Chem.* **2002**, *12*, 500–510.
(43) Trofimov, B. A.; Mikhaleva; A. I. In *N-Vinylpyrroles*; Voronkov, M. G., Ed.; Nauka: Novosibirsk, 1984.
(44) Roncali, J. *Chem. Rev.* **1992**, *92*, 711–738.
(45) Charge in percolation in electroactive polymers. In *Electroactive Polymer Chemistry, Part 1 Fundamentals*; Lyons, M. E. G.; Plenum Press: New York, 1994.
(46) Asensio, J. A.; Borrós, S.; Gómez-Romero, P. *J. Polym. Sci.: Part A: Polym. Chem.* **2002**, *40*, 3703–3710.
(47) Kiebooms, R.; Aleshin, A.; Hutchison, K.; Wudl, F.; Heeger, A. *Synth. Met.* **1999**, *101*, 436–437.
(48) Cho, J. W.; Han, M. G.; Kim, S. Y.; Oh, S. G.; Im, S. S. *Synth. Met.* **2004**, *141*, 293–299.
(49) Mastragostino, M.; Arbizzani, C.; Ferloni, P.; Marinangeli, A. *Solid State Ionics* **1992**, *53*, 471–478.
(50) Gaupp, C. L.; Welsh, D. M.; Rauh, R. D.; Reynolds, J. R. *Chem. Mater.* **2002**, *14*, 3964–3970.
(51) CIE, Colorimetry (Official Recommendations of the International Commission on Illumination), CIE Publication No. 15, Paris, 1971.
(52) Holland, D. M. P.; Karlson, L.; Nisson, V. W. *J. Electron Spectrosc. Relat. Phenom.* **2001**, *113*, 221–239.
(53) Trofimov, A. B.; Zaytzeva, I. L.; Holland, D. M. P.; Schirmer, J.;to be published.
(54) Alemán, C.; Domingo, V. M.; Fajari, L.; Juliá, L.; Karpfen, A. *J. Org. Chem.* **1998**, *63*, 1041–1048.
(55) Becke, A. D. *J. Chem. Phys.* **1993**, *98*, 5648–5652.
(56) Lee, C.; Yang, W.; Parr, R. G. *Phys. Rev. B.* **1988**, *37*, 785–789.
(57) Krisnan, R.; Binkley, J. S.; Seeger, R.; Pople, J. A. *J. Chem. Phys.* **1980**, *72*, 650–654.
(58) Schmidt, M. W.; Baldridge, K. K.; Boatz, J. A.; Elbert, S. T.; Gordon, M. S.; Jensen, J. H.; Koseki, S.; Matsunaga, N.; Nguyen, K. A.; Su, S. J.; Windus, T. L.; Dupuis, M.; Montgomery, L. A. *J. Comput. Chem.* **1993**, *14*, 1347–1363.

MA801190N